

Spring 1996

A simulation environment for CDMA wireless communication systems in AWGN channels

Muzaffer Kanaan
New Jersey Institute of Technology

Follow this and additional works at: <https://digitalcommons.njit.edu/theses>



Part of the [Electrical and Electronics Commons](#)

Recommended Citation

Kanaan, Muzaffer, "A simulation environment for CDMA wireless communication systems in AWGN channels" (1996). *Theses*. 1063.

<https://digitalcommons.njit.edu/theses/1063>

This Thesis is brought to you for free and open access by the Electronic Theses and Dissertations at Digital Commons @ NJIT. It has been accepted for inclusion in Theses by an authorized administrator of Digital Commons @ NJIT. For more information, please contact digitalcommons@njit.edu.

Copyright Warning & Restrictions

The copyright law of the United States (Title 17, United States Code) governs the making of photocopies or other reproductions of copyrighted material.

Under certain conditions specified in the law, libraries and archives are authorized to furnish a photocopy or other reproduction. One of these specified conditions is that the photocopy or reproduction is not to be “used for any purpose other than private study, scholarship, or research.” If a user makes a request for, or later uses, a photocopy or reproduction for purposes in excess of “fair use” that user may be liable for copyright infringement,

This institution reserves the right to refuse to accept a copying order if, in its judgment, fulfillment of the order would involve violation of copyright law.

Please Note: The author retains the copyright while the New Jersey Institute of Technology reserves the right to distribute this thesis or dissertation

Printing note: If you do not wish to print this page, then select “Pages from: first page # to: last page #” on the print dialog screen

The Van Houten library has removed some of the personal information and all signatures from the approval page and biographical sketches of theses and dissertations in order to protect the identity of NJIT graduates and faculty.

ABSTRACT

A SIMULATION ENVIRONMENT FOR CDMA WIRELESS COMMUNICATION SYSTEMS IN AWGN CHANNELS

by
Muzaffer Kanaan

The goal of this work is the development of a wireless communication system simulator. The simulator has been developed primarily to aid in the studies of Code Division Multiple Access (CDMA) digital cellular systems. We begin by introducing the fundamentals of spread spectrum communications and the motivation for this work. We then take a detailed look at CDMA systems and their structure. We then verify the accuracy of the simulator by using it to simulate some familiar system scenarios. We end this work by presenting conclusions and suggestions for further work.

A SIMULATION ENVIRONMENT FOR CDMA WIRELESS
COMMUNICATION SYSTEMS IN AWGN CHANNELS

by
Muzaffer Kanaan

A Thesis
Submitted to the Faculty of
New Jersey Institute of Technology
in Partial Fulfillment of the Requirements for the Degree of
Master of Science in Electrical Engineering

Department of Electrical and Computer Engineering

May 1996

BIOGRAPHICAL SKETCH

Author: Muzaffer Kanaan
Degree: Master of Science
Date: May, 1996

Undergraduate and Graduate Education:

- Master of Science in Electrical Engineering,
New Jersey Institute of Technology, Newark, NJ, 1996
- Bachelor of Science in Electrical Engineering,
Eastern Mediterranean University, Famagusta, North Cyprus, 1994

Major: Electrical Engineering

This work is dedicated to
my family

ACKNOWLEDGMENT

I would like to thank a number of people who have made significant contributions to the development of this thesis. To begin with, I would like to thank my advisor Dr. Zoran Siveski who has provided me with a lot of knowledge and encouragement. I would also like to thank Dr. Ali Akansu and Dr. Nirwan Ansari for serving on my thesis evaluation committee. I would also like to express my sincere gratitude and thanks to Lisa Fitton, Administrative Assistant at the Center for Communications and Signal Processing Research, NJIT, for her helpful comments about the appearance of the thesis and her jovial personality which made working at the lab a very enjoyable experience. Sincere thanks are also due to Ms. Annette Damiano of the Graduate Studies Office at NJIT for her efforts to enhance the overall professional quality of the document.

Several of my colleagues at the lab are deserving of recognition for their help at one point or another. I would like to thank past graduates Dr. Nadir Sezgin, Dr. Mehmet Tazebay and Murat Berin for all the helpful discussions that we have had regarding the various points in the thesis. I also thank Ambalavanar Arulambalam (for his help with C language and \LaTeX), Amit Shah and Shahid Rana (for their witty personality which made those final tense moments easier to bear), Ashwini Borkar and Nico Van Waes, Sudhakar Thiagarajan and Huaping Liu.

Last, but not least, I would like to thank my parents whose support and help was never in short supply. It is my sincere belief that, without their unwavering encouragement, this work would never have come to fruition.

TABLE OF CONTENTS

Chapter	Page
1 INTRODUCTION	1
1.1 Chapter Overview	1
1.2 Spread Spectrum Communications	1
1.3 Direct Sequence Spread Spectrum	3
1.4 Motivation Behind This Work	5
2 CDMA SYSTEM CONCEPTS	7
2.1 Chapter Overview	7
2.2 CDMA for Wireless Cellular Networks	7
2.3 Capacity Issues in Cellular CDMA	14
2.4 Power Control in CDMA	20
2.5 Error-Correction Coding Aspects of CDMA Systems	22
3 SIMULATION RESULTS	34
3.1 Chapter Overview	34
3.2 Simulation Results	34
4 CONCLUSIONS & SUGGESTIONS FOR FURTHER WORK	42
4.1 Chapter Overview	42
4.2 Conclusions on Results	42
4.3 Suggestions for Further Work	43
REFERENCES	44

LIST OF TABLES

Table	Page
2.1 Comparison of different cellular systems	20

LIST OF FIGURES

Figure	Page	
1.1	Signal waveforms in a spread spectrum system. (a) The original data sequence, $m(t)$. (b) The spreading sequence, $c(t)$. (c) The spread spectrum signal, $s(t) = m(t)c(t)$. The processing gain $N = 5$	4
1.2	Power spectral density plots showing the effect of spread spectrum modulation on a signal.	5
2.1	FDMA channelization	8
2.2	TDMA channelization	9
2.3	CDMA channelization	11
2.4	Illustrating the frequency concept with $N = 7$ (seven-cell pattern)	12
2.5	An example single-cell configuration used to discuss the problems of multiple access interference and near-far effect in cellular CDMA	13
2.6	Generic CDMA mobile terminal modem structure	16
2.7	Generic CDMA cell-site transmitter/receiver structure. The constants $\alpha_1, \dots, \alpha_N$ are scaling constants used for power control purposes.	17
2.8	Cell sectorization.	18
2.9	The fundamentals of block coding.	23
2.10	A 4-state convolutional encoder	24
2.11	A 256-state convolutional encoder	25
2.12	The concept of free distance	27
2.13	The concept of soft-decision decoding	28
2.14	State diagram for a rate-1/2, $K = 3$ convolutional encoder	29
2.15	Trellis diagram for the 4-state encoder	30
2.16	The block interleaver	32
2.17	The block deinterleaver	33
3.1	A two-user simulation with and without error-control coding	35
3.2	Error performance of the desired user with differing levels of multiple-access interference (hard-decision decoding)	36

LIST OF FIGURES
(Continued)

Figure	Page
3.3 Error performance of the desired user with differing levels of multiple-access interference (soft-decision decoding)	37
3.4 Error performance of the desired user with differing levels of path-loss (hard-decision decoding)	38
3.5 Error performance of the desired user with differing levels of path-loss (soft-decision decoding)	39
3.6 Error performance of the desired user in a multiuser environment	40

CHAPTER 1

INTRODUCTION

1.1 Chapter Overview

In this chapter, we shall discuss the fundamental principles of spread spectrum communications. We shall give a definition of spread spectrum and also examine why it is considered an attractive signaling scheme for certain communication scenarios. This fundamental foundation will set the stage for the discussion of the Code Division Multiple Access (CDMA) digital cellular systems in the next chapter. Finally, we shall present the fundamental motivation behind the present work.

1.2 Spread Spectrum Communications

Basically, spread spectrum is a digital transmission technique where the data sequence occupies a bandwidth far larger than the minimum bandwidth required to send it [11]. The resulting wideband signal will not interfere with any other signal operating in the same frequency band [4].

By virtue of this definition, spread spectrum is not a bandwidth-conserving modulation technique. However, it still finds wide application because of its ability to solve two important communications problems [9]. One of these problems is to lower the probability of unauthorized signal detection, which is a particularly serious problem for military communications. The designer of such a system would aim for a design that would minimize this probability. As it turns out, spread-spectrum techniques can greatly aid the system designer towards the attainment of this goal. This is possible because, as a result of spectrum spreading, the power spectral density of the signal to be transmitted goes down to a level that is below the thermal noise level of the unfriendly receiver [4]. This simply means that the spread spectrum will be perceived by any other unauthorized receiver as noise. The second problem is the signal degradation caused by jamming and interference. Here spread spectrum

signaling reduces the overall power of the interference so that communication can take place.

Although spread spectrum techniques were initially developed exclusively for military applications, in recent years, the commercial applications of these techniques are gaining increasing significance. Perhaps the best example lies in the area of mobile communications, where spread spectrum techniques are being used for the Code Division Multiple Access (CDMA) digital cellular system. As is well known, cellular market is one of the fastest-growing areas of mobile communications. The ever-increasing number of users in the cellular band has prompted the mobile communications industry to search for more spectrally efficient signaling schemes that would:

- enable more users to share the same spectrum;
- still maintain an acceptable quality of service.

CDMA has been proven to offer capacity increases (in terms of the maximum number of users supportable without degradation in the quality of service) over other types of cellular networks such as Time Division Multiple Access (TDMA) networks and Frequency Division Multiple Access (FDMA) networks. Indeed, CDMA seems to be so attractive that it is being hailed as the best infrastructure platform, both for next-generation cellular networks and for future Personal Communication Systems (PCS). Because of its potential, the Telecommunications Industry Association (TIA) has recently released a new interim standard for CDMA, known as IS-95.

There are two types of spread spectrum signaling: *direct sequence* and *frequency hopping*. Direct sequence spread spectrum is usually used with some form of digital phase modulation such as BPSK, DPSK or MPSK. Frequency hopping spread spectrum is usually employed with some form of digital frequency modulation such as MFSK. Because of its relevance in the IS-95 standard, we shall ignore frequency-hopping in this presentation and concentrate exclusively on direct sequence spread

spectrum. We discuss direct sequence spread spectrum (DSSS) systems in the next section.

1.3 Direct Sequence Spread Spectrum

In direct sequence spread spectrum, the data sequence is spread by a spreading code. This is achieved by simply multiplying every bit in the data sequence $m(t)$ by the spreading code $c(t)$ as shown in fig. 1.1.

As can be seen from fig. 1.1. the spreading sequence $c(t)$ has a much higher bit rate than the original data sequence. The bit rate of the spreading sequence is known as *chip rate*. As a result of this operation, the bandwidth of the transmitted signal becomes higher and the power level goes down as shown in the power spectral density plot of fig. 1.2. If we assume that the total power transmitted by the spread spectrum signal is the same as that in the original narrowband signal [10]. Then the power spectral density, P_{ss} , of the spread spectrum signal can be expressed as:

$$P_{ss} = P_s \left(\frac{B_s}{B_{ss}} \right) \quad (1.1)$$

where P_s is the power spectral density of the original signal, B_s is the bandwidth occupied by the original signal and B_{ss} is the bandwidth occupied by the spread spectrum signal. The ratio B_{ss}/B_s is known as the *processing gain* of the system. Numerically, it is equal to the length of the spreading code. For example, in fig. 1.1, the original signal is spread by multiplying it with a spreading sequence of length 5. Therefore, the processing gain for this system is 5. For most practical systems, this parameter takes on values in the range 10–30 dB. This means that the power of the original signal is spread over a bandwidth 10–1000 times the original signal bandwidth, while its power spectral density is reduced by the same factor [10].

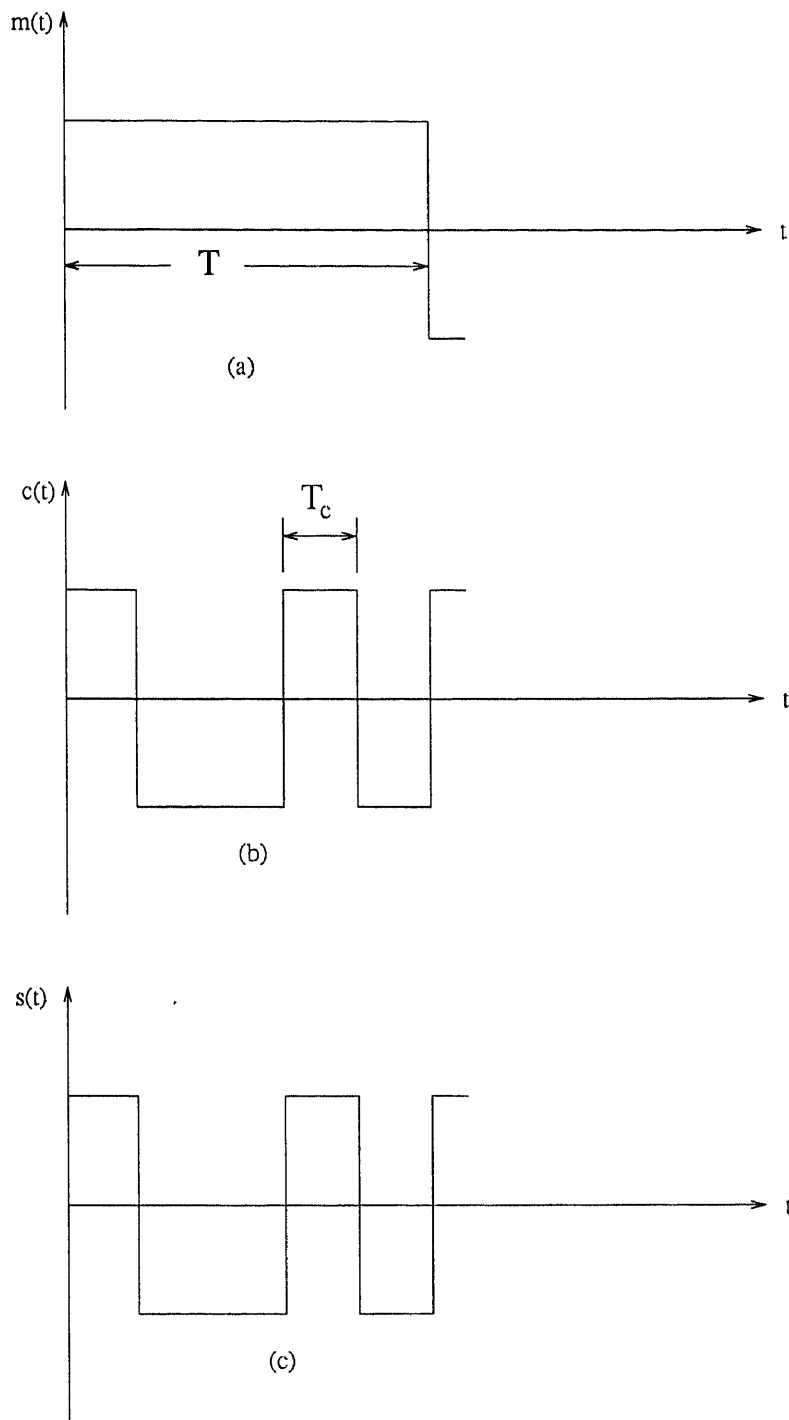


Figure 1.1 Signal waveforms in a spread spectrum system. (a) The original data sequence, $m(t)$. (b) The spreading sequence, $c(t)$. (c) The spread spectrum signal, $s(t) = m(t)c(t)$. The processing gain $N = 5$.

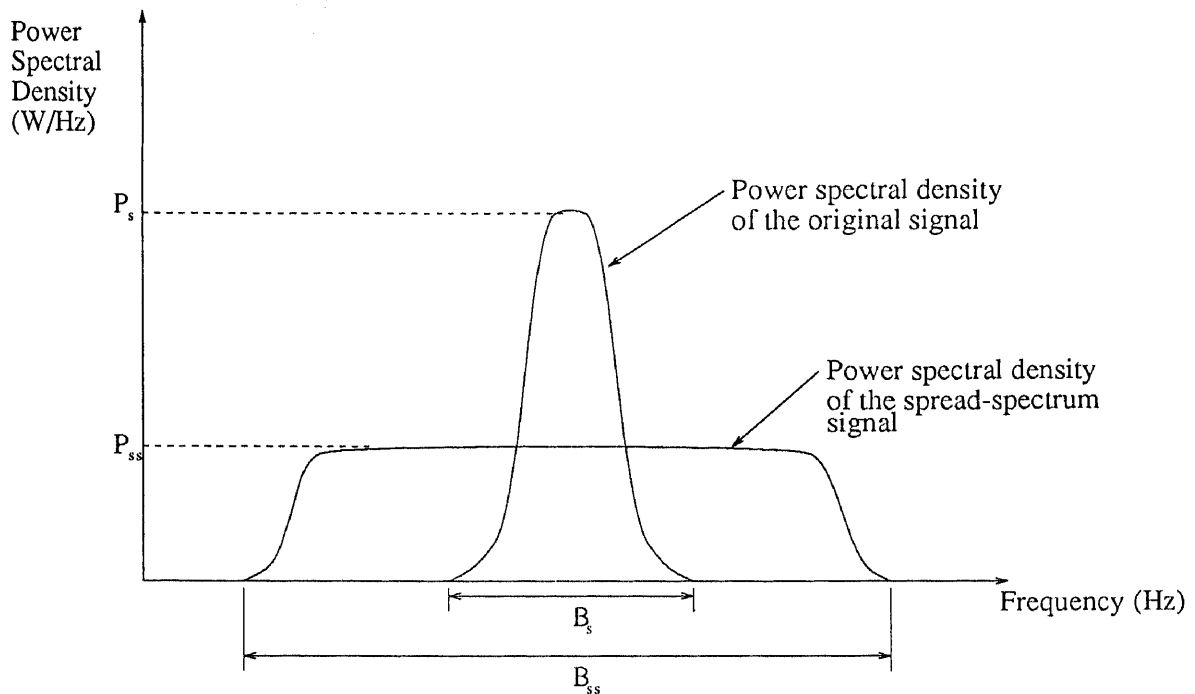


Figure 1.2 Power spectral density plots showing the effect of spread spectrum modulation on a signal.

1.4 Motivation Behind This Work

As was already mentioned above, the cellular industry is growing at an explosive pace. Cellular service providers and equipment manufacturers are faced with the challenge of catering for the needs of an ever-increasing number of subscribers who demand better service and coverage. This requires extensive research effort, on the part of both of service providers and equipment manufacturers, to improve their networks so that an increasing number of users can be supported without sacrificing on the quality of service (particularly signal quality and coverage). CDMA is widely accepted as a good solution to this multi-faceted problem.

In recent years, design of many engineering systems has become increasingly more computer-oriented. Computer simulation is being used increasingly more often in the design process, both to check the validity of a design or to discover potential problems that could arise if the design is implemented. It is a cost-effective way to

verify and test a design without having to build an actual prototype of the system itself. The aim of this thesis was to develop such a simulation tool to be used in design and performance evaluation studies of CDMA systems. The simulator is highly modular in nature. Because of this, it is easily extensible and can be used to simulate systems with varying degrees of complexity with little or no modification. The simulator has been tested by using it to simulate some familiar system scenarios and it has been found to perform accurate simulations in fairly short time. The results and their interpretation will be presented in chapter 3.

CHAPTER 2

CDMA SYSTEM CONCEPTS

2.1 Chapter Overview

In this chapter, we shall use the fundamental foundations of spread spectrum systems to discuss Code Division Multiple Access (CDMA) digital cellular systems. We shall examine the various characteristics of these systems that make them attractive against other digital cellular systems like Time Division Multiple Access (TDMA) and Frequency Division Multiple Access (FDMA) systems. We shall also examine the various problems with CDMA systems and the various modulation and coding approaches to mitigate them. In the course of the presentation, we shall draw examples from a practical system, the IS-95 CDMA system, to illustrate the concepts at hand.

2.2 CDMA for Wireless Cellular Networks

In the design of every cellular system, system designers face the multi-faceted problem of *multiple access*. Basically, this can be characterized as a filtering problem [13]. There are a number of mobile users who wish to make use of the same region of the electromagnetic spectrum. The problem is to come up with an arrangement of filtering and other signal processing techniques so that the following two objectives will be achieved:

- signals from different users can be separately received and demodulated;
- within any given user signal, the interference from other users can be reduced to a minimum.

Towards this end, a number of different multiple access schemes have been devised. Three of the most prevalent of these are Frequency Division Multiple Access

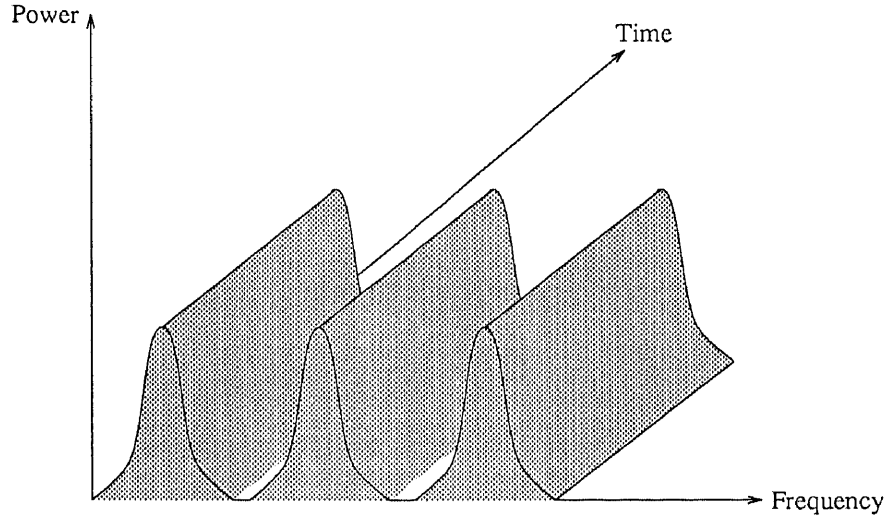


Figure 2.1 FDMA channelization

(FDMA), Time Division Multiple Access (TDMA) and Code Division Multiple Access (CDMA).

In FDMA, each user is given a certain slice of the frequency band. In this scheme, each user is free within their frequency band any time they please. It is a straightforward way of sharing RF bandwidth resources among multiple users in an equitable manner. This scheme, however, has the problem that a certain *guard band* needs to be set between different user channels to minimize the well-known phenomenon of *crosstalk*. This is obviously wasteful of bandwidth. The capacity (that is, the maximum number of users that can be supported without degrading the quality of service) of such a system is limited by the total bandwidth available. The basic concept of FDMA is shown in fig 2.1.

TDMA was developed to remedy the capacity shortcomings of the FDMA system. This system works on the same channel assignments as FDMA. However, it also incorporates the idea of sharing the channels in time. In the present systems, each channel is shared in time by three users. This effectively triples system capacity;

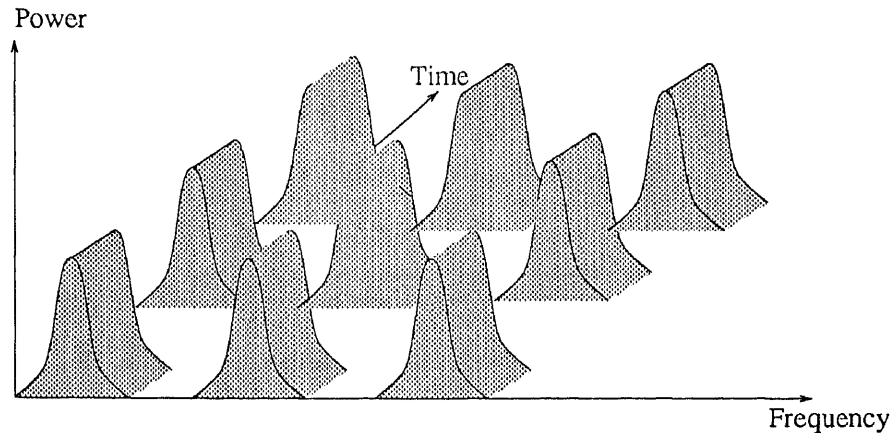


Figure 2.2 TDMA channelization

however, the necessity of setting the guard band still remains and the upper bound to capacity is again the available system bandwidth. TDMA forms the basis for all the digital cellular systems in use today, including the widely-used European standard GSM (Global System for Mobile Communications). The concepts of TDMA method are illustrated in the fig 2.2.

CDMA is radically different from both of these systems because here all the users have access to all the spectrum all the time. This is possible because, in this system every user is identified by a unique code sequence, sometimes referred to as a *signature sequence*. Because of this, if we examine CDMA signals in time or frequency, we would see them to be on top of one another. The idea is shown, in a highly simplified form, in the fig 2.3. CDMA is also different from others in that it does not need to employ *frequency reuse*. The concept of frequency reuse can be explained in the following way. Radio waves propagating throughout a cell exhibit the well-known phenomenon of *path loss* where the power level of the RF signal decreases inversely with some power of the distance r as given by:

$$P_r = \frac{P_t}{r^n} \quad (2.1)$$

where P_t is the power transmitted by the mobile (or the base station), P_r is the power received at the base station (or the mobile) and r is the distance between them. Equation 2.1 hold true for both base-to-mobile link (or downlink) and the mobile-to-base link (or uplink). The exponent n is usually taken to be between 2 and 4, depending on the propagation model used to describe the channel. For instance, in cellular systems, terrestrial UHF propagation model is used, for which $n = 4$ [6]. This means that if a particular frequency band is being used in a certain cell, that same frequency band can be *reused* on another cell, provided that the distance between the two cells is large enough. In order to minimize co-channel interference, channels allocated for a given geographic area are divided into N distinct sub-channels and each sub-channel is assigned to one cell in a group of N cells [9]. The number N is known as the *frequency reuse factor* of the cellular system. It is dependent on a number of factors, such as the degree of immunity, of the modulation, coding and diversity techniques employed, to co-channel interference. The current cellular systems use $N = 7$. The idea is illustrated in fig 2.4. Since the CDMA system distinguishes individual users by their signature sequences, the same spectrum can be utilized in all cells. This will increase the overall system capacity by a large percentage of the frequency reuse factor [6]. The capacity issues of CDMA will be considered in detail in the next section.

Besides the capacity increase issues briefly mentioned above, CDMA has two other advantages which are worthy of our attention. The first is the communications privacy that CDMA provides as a result of the spread spectrum modulation. The second is its ability to combat the effects of multipath fading. Because the CDMA signal is wideband, its bandwidth will be greater than the *coherence bandwidth* of the channel, defined as in [8]. As a result, different frequency components will be affected differently by the multipath fading channel. In this way, the receiver can easily distinguish or resolve the separate multipaths. These multipaths can then be

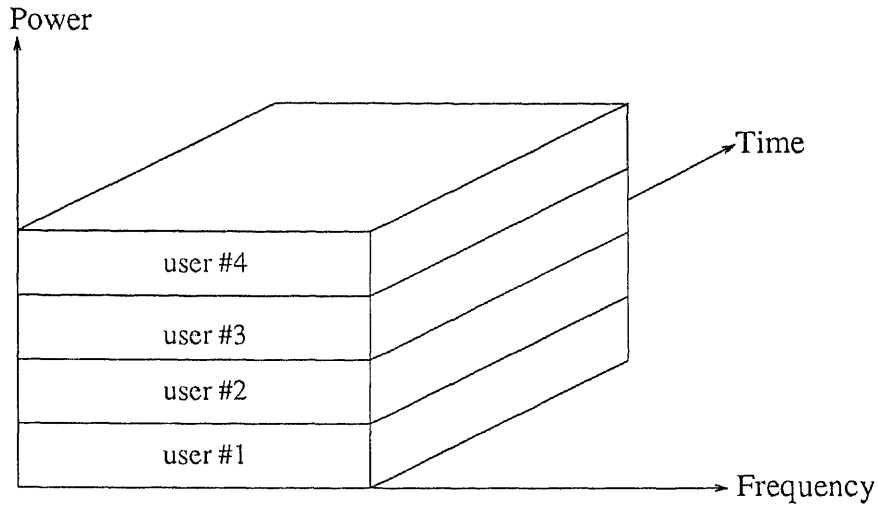


Figure 2.3 CDMA channelization

separately processed and combined in an optimal manner (as in a RAKE receiver [8]) to enhance the error performance of the system. This is clearly a form of diversity that provides the receiver with several independently fading signal paths [8].

However, despite all the advantages that it offers, CDMA is not without its problems. The problems with CDMA can be considered under two headings: *multiple-access interference* and the *near-far effect*. Actually, these two problems are very closely related and thus cannot be considered as separate problems. To illustrate the connection, consider the scenario depicted in fig 2.5. Here we have two mobiles, $M1$ and $M2$, both trying to communicate with the base station (BS). The mobiles are at distances $d1$ and $d2$ respectively. For the first user, the signal received at the base station at any time instant t is:

$$r_1(t) = \sqrt{a_1}c_1(t)b_1(t) + \rho_{12}\sqrt{a_2}c_2(t)b_2(t) + n_1(t) \quad (2.2)$$

For the second user, the received signal at the base station is:

$$r_2(t) = \sqrt{a_2}c_2(t)b_2(t) + \rho_{12}\sqrt{a_1}c_1(t)b_1(t) + n_2(t) \quad (2.3)$$

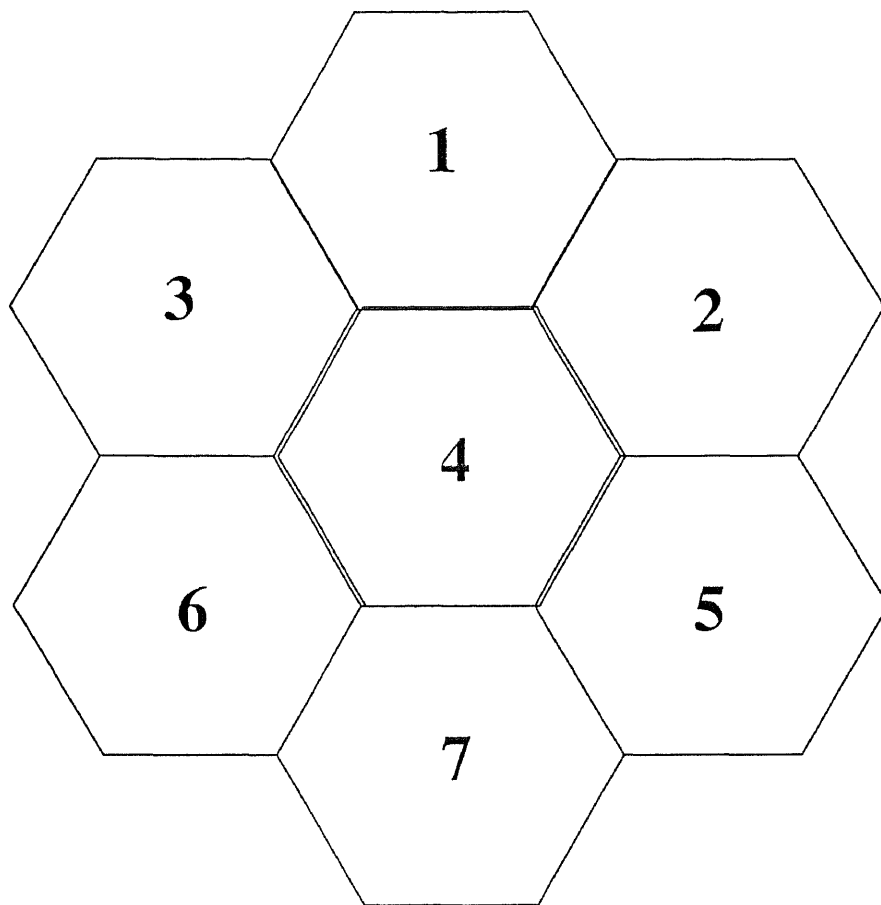


Figure 2.4 Illustrating the frequency concept with $N = 7$ (seven-cell pattern)

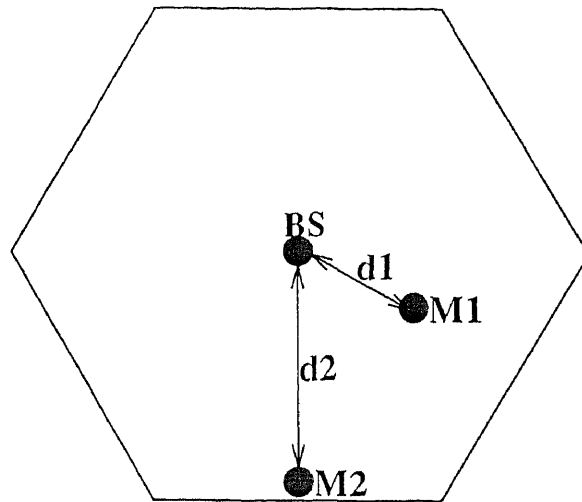


Figure 2.5 An example single-cell configuration used to discuss the problems of multiple access interference and near-far effect in cellular CDMA

In the equations 2.2 and 2.3, $c_1(t)$ and $c_2(t)$ represent the complex channel attenuation (or gain) that affect the user signals $b_1(t)$ and $b_2(t)$ respectively. The amplitudes of $c_1(t)$ and $c_2(t)$ are usually modeled as Rayleigh-distributed random variables and their phases are modeled as uniformly-distributed random variables. ρ_{12} represents the cross-correlation coefficient between the signature sequences of the two users. $n_1(t)$ and $n_2(t)$ simply represent white gaussian noise. The second term of both equations represents the multiple access interference, caused by the non-zero cross-correlation between the signature sequences. Let us now assume that $M2$ is the desired user. Since $M1$ is closer to the base station than $M2$, its signal will be received at a higher power level than that of $M2$. This means that the desired user's signal will be received with a significant amount of interference. In this way, the multiple-access interference problem is further increased by the near-far effect. Note that if $\rho_{12} = 0$ then these problems will cease to exist. In practice, however, it is difficult to find code sequences that are perfectly orthogonal. Even if such families of codes are found, the time-delays introduced by the multipath fading channels

will destroy the orthogonality. However, codes with quite good cross-correlation properties have been found and the usage of these codes, along with stringent power control, can combat this problem and bring system performance within acceptable limits. Power control is essential for the proper operation of a cellular CDMA system and will be discussed in detail in a later section. For now, we shall turn our attention to the capacity increase issues of cellular CDMA systems. This is the topic of the next section.

2.3 Capacity Issues in Cellular CDMA

As was already mentioned in the last section, CDMA capacity is limited by interference, rather than by bandwidth (as is the case in FDMA or TDMA). By interference, we mean multiple-access interference. Therefore, the issue of increasing capacity in a CDMA system is exactly equivalent to the issue of reducing this interference because any reduction in interference would translate into a capacity increase [6]. One way of reducing the interference is to take advantage of the intermittent nature of voice signals. It has been statistically observed that, in a typical phone conversation, each user is active only 37.5% of the time. This corresponds to a *duty factor* of 3/8 [2]. Because of this, during the idle periods, transmission can be suppressed for a user and the channel made available for another user. This kind of dynamic channel sharing among multiple users has been shown to increase CDMA system capacity by an amount inversely proportional to the speech activity factor [6].

We have already seen in the previous section that CDMA, by the virtue of spread spectrum techniques, does not need to reuse frequencies in any cell. Therefore, the same frequencies can be reused in all cells. Therefore, the maximum number of users supportable per cell goes up by a large percentage of the normal frequency reuse factor (which is 7 in present systems) [6], but is nevertheless limited by multiple access interference.

We shall now present some quantitative results of analyses on CDMA capacity. This issue is especially well-documented in the literature, particularly in [7] and [6]. We shall start by considering a single-cell scenario, illustrated in fig 2.5. We assume a generic CDMA modem structure as shown in fig 2.6 for the mobile terminal. As such, we have an encoder (to correct random errors introduced by the channel) and an interleaver (which will combat the burst of errors introduced by the fading channel) which collectively constitute the forward-error correction (FEC) coding block. This is followed by a stage that performs the spreading. Finally we have a stage that implements the analog amplification and carrier modulation (marked as "Carrier Modulation" in fig 2.6). In fig 2.7, we show a generic structure of a CDMA cell-site transmitter. This incorporates a linear combiner that sums a number of signals that come from the users. Each user signal is weighted by a factor α_i ($i = 1, \dots, N$) in accordance with the power control requirements. Based on these structures, a capacity analysis for the single-cell system can be made. With power control, it can be assured that all the user signals will be received at the same power level. Therefore, the cell-site receiver has to process one desired signal having power S and $N - 1$ interfering users, each of which also has power S by virtue of power control. Remaining fully consistent with the notation of [6], the capacity in terms of N , the number of users supported, can be written as:

$$N = 1 + \frac{W/R}{E_b/N_0} - \frac{\eta}{S} \quad (2.4)$$

where:

W : total bandwidth of the spread signal

R : information bit rate

η : variance of the thermal noise, as well as spurious interference components (such as man-made interference) contained in the total spread bandwidth, W .

E_b/N_0 : bit energy-to-noise-density ratio required by the modem and the decoder.

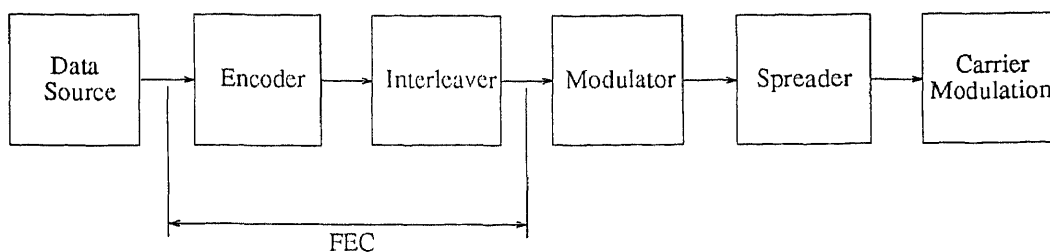


Figure 2.6 Generic CDMA mobile terminal modem structure

This value depends, to a large extent, on the robustness of the modulation and error-correction coding techniques used.

From this equation, we can solve for E_b/N_0 to yield the following equation:

$$E_b/N_0 = \frac{W/R}{(N - 1) + (\eta/S)} \quad (2.5)$$

From equation 2.4, we can easily see that, if the value of E_b/N_0 required for proper operation can be lowered, then capacity can be increased. This can be done through better modulation and coding but this will increase the complexity of the receiver. Also, this approach will rapidly lead to a point where any further increase in complexity is simply not accompanied by a corresponding increase in performance, and ultimately to the unattainable Shannon limit. There are two other solutions to this problem:

1. Cell sectorization.
2. Voice-activity monitoring.

In cell sectorization, directional antennas are used at the cell-site for both transmitting and receiving. This technique is usually applied in practice by using 3 antennas at the cell-site, each with 120° effective beamwidths (see fig 2.8). This will, in effect, lower the number of interferers seen by any antenna (characterized by the $N - 1$ in the denominator of equation 2.5 by a factor of 3 (as compared to an omnidirectional antenna). As a result, the $(N - 1)$ factor in equation (2.5) (which

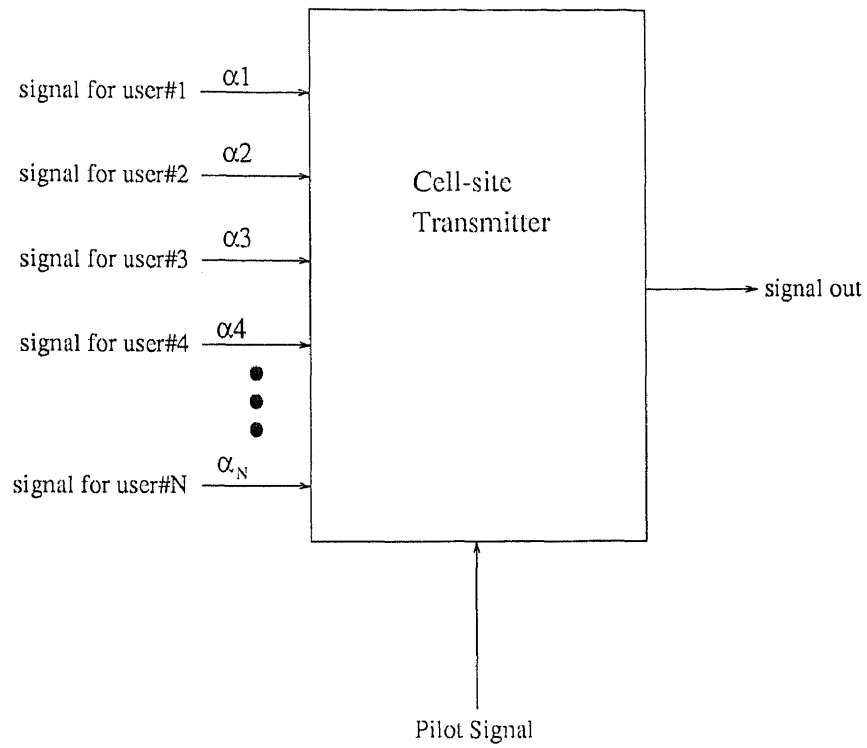


Figure 2.7 Generic CDMA cell-site transmitter/receiver structure. The constants $\alpha_1, \dots, \alpha_N$ are scaling constants used for power control purposes.

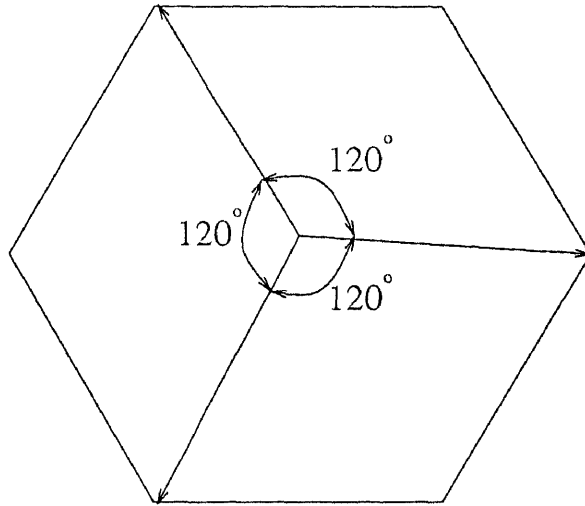


Figure 2.8 Cell sectorization.

characterizes the interfering users) will be reduced by a factor of 3 and consequently in equation 2.4 will be increased by a factor close to 3. Using three sectors (120° sectorization) we find that the number of users supportable per cell can be written as $N = 3N_s$, where N_s is the number of users per sector [6].

In voice-activity monitoring, the vocoder could be designed such that transmission can be suppressed for a user when there is no speech activity detected. This solution has already been integrated into the IS-95 CDMA standard [16] in the form of a variable-rate speech coder that transmits data at 9600, 4800, 2400 or 1200 bps based on the measurements of speech activity. This makes more efficient use of the bandwidth and also reduces the interference which, in turn, increases capacity. The average E_b/N_0 (denoted by $\overline{E_b}/N_0$) which incorporates the effects of sectorization and voice-activity monitoring, is given by

$$\frac{\overline{E_b}}{N_0} = \frac{W/R}{(N_s - 1)\alpha + (\eta/S)} \quad (2.6)$$

where α is the speech-activity factor.

The implications of the above equation can be explained by comparing it to

equation 2.5. Comparing the two equations, we note that the factor $(N_s - 1)\alpha < (N - 1)$. From practical considerations, it has been established that, with two-antenna diversity and a powerful error-correcting code (such as a rate-1/3 constraint length 9 convolutional code), an E_b/N_0 value of 7 dB is necessary for acceptable error performance (assumed as $BER < 10^{-3}$ for digital voice transmission [6]). If we equate the two equations, we find that the number of users can be increased while still maintaining acceptable performance. It is estimated in [6] that the capacity increase factor (even when fading is considered) will be 5 or 6.

The treatment of the multiple-cell case is quite complicated. Therefore, we shall contend ourselves with presenting a few end-results and taking a look at their interpretation; full details can be obtained from [6]. For the reverse link, the capacity is expressed in terms of P , the probability of obtaining $BER < 10^{-3}$, in terms of the number of users. This, in effect, is a lower bound on the performance. This is a good way of expressing the result because it would also give a quantitative idea of how much the performance degradation would be if the number of users were increased. The result has been derived as

$$P = 1 - \sum_{k=0}^{N_s-1} \binom{N_s-1}{k} \alpha^k (1-\alpha)^{N_s-1-k} Q\left(\frac{\delta - k - 0.247N_s}{\sqrt{0.078N_s}}\right) \quad (2.7)$$

where:

N_s : number of users per sector (assuming 120° sectorization)

α : voice-activity factor

E_b/N_0 : taken to be 5 (corresponding to 7 dB, a value that gives acceptable performance as discussed above).

$$\delta = \frac{W/R}{E_b/N_0} - \frac{\eta}{S}$$

$$Q(x) = \frac{1}{\sqrt{2\pi}} \int_x^{\infty} e^{-z^2/2} dz$$

Table 2.1 Comparison of different cellular systems

Scheme	Total number of channels	Frequency reuse factor	Radio capacity (channels/cell)
FDMA	41.67	7	6
TDMA	125	4	31.25
CDMA	13	1.33	120

As for the forward link, such an analytical derivation is not possible and the only solution is through Monte-Carlo simulation [6]. We will not concern ourselves any more with the details but simply cite some significant results, both for the forward link and the reverse link. Assuming $W = 1.25$ MHz, $R = 8$ kb/s and $\alpha = 3/8$, it is found from equation 2.7 that the reverse link can support over 36 users/sector or 108 users/cell with $BER < 10^{-3}$ more than 99% of the time. For the same choice of parameters, it has been found through simulation that the forward link can support about 38 users/sector or 114 users/cell with the same level of performance. It should be stressed that all these results assume some form of accurate power control.

Having thus examined various aspects of CDMA that make it superior in terms of capacity, it is now instructive to compare its capacity to the capacity of TDMA and FDMA systems on a quantitative basis. A generally applicable method to compare the three systems does not exist in the literature. However, a more or less unified comparison is presented in [7]. We summarize the results in table 2.1.

2.4 Power Control in CDMA

As was already mentioned, power control is one of the most fundamental components of any CDMA cellular system. Due to the signaling structure employed by CDMA, each user's signal is interference to the other users. The presence of the near-far problem will give rise to substantial amounts of co-channel interference because all

the users are sharing the same channel and a desired user's signal can be received with a lot of interference. In order to minimize this interference, power control is required. As a result, capacity will be increased. A less obvious benefit is the following. Since power control allows all users' signal power to be received at the same level, each user will be required to transmit only enough power to maintain a certain level of error performance [1]. This means that the portable units can be operated at low power, which prolongs battery life and can even alleviate the recent health concerns arising from cellular phone radiation.

There are two types of power control used in CDMA systems: *open-loop* and *closed-loop* power control. Both have been incorporated into the CDMA standard, IS-95 and will be separately discussed in the following.

The basic idea behind open-loop power control is the similarity of the power loss (or attenuation) in the forward link and the reverse link [16]. The reference power level is taken to be the power received at the mobile station. If the mobile station receives a signal at a lower power level, it assumes that it is far away from the base station and therefore it will transmit at a higher power level. The product of the two power levels (or their sum if the powers are measured in dB) is equated to a constant. According to the present IS-95 standard, this constant is -73 dBm. Therefore, if the received power level is, say, -75 dBm, then the transmitted power level is +2 dBm.

Closed-loop power control, as its name implies, utilizes a feedback structure to achieve the same end-result. In this case, the reference power level is specified by the base station. Here, the idea is to force the power level transmitted by the mobile to deviate from the open-loop setting [16]. The base station periodically sends control information to the mobile, directing it to either raise or lower its power by a fixed increment. According to the present IS-95 standard, the base station has to send this control information at 1.25-millisecond intervals and the power increment is 1

dB. It is a very effective way of regulating the mobile-station power. However, in fast-fading channels, the feedback delay encountered may be large enough to render it impractical.

2.5 Error-Correction Coding Aspects of CDMA Systems

A full discussion of cellular CDMA systems would not be complete without a treatment of the error-correction coding aspects of the systems. CDMA systems, like any other cellular system, must operate in an adverse channel environment caused by such detriments as fading and shadowing. In order to counter these detriments, CDMA systems must incorporate some form of error-correction coding. This makes error-correction coding a central issue in overall system design.

By its nature, error-correction coding involves adding redundancy to the original information bit for the purpose of detecting and correcting errors. For a non-spread-spectrum system, this means that either the transmission bandwidth has to be increased to accommodate these other redundant bits or the information bit rate has to be decreased so that the overall transmission bandwidth requirements stay the same after adding the redundancy. However, as proved in [15], this does not hold true for spread spectrum systems. Moreover, it is also proved in [15] that the redundancy brought about by error-correction coding does not decrease the processing gain.

Error-correction coding algorithms can be classified into two basic classes: *block coding* and *convolutional coding*. Each has got a unique set of applications for which it is suited. We present a brief overview of both disciplines below.

In block coding, the data bit stream is organized into fixed-size blocks and some extra bits are added to the block by means of a predefined algorithm. This can be thought of as a mapping from a vector of k uncoded bits $\mathbf{c} = \{c_0, c_1, c_2, \dots, c_k\}$ to

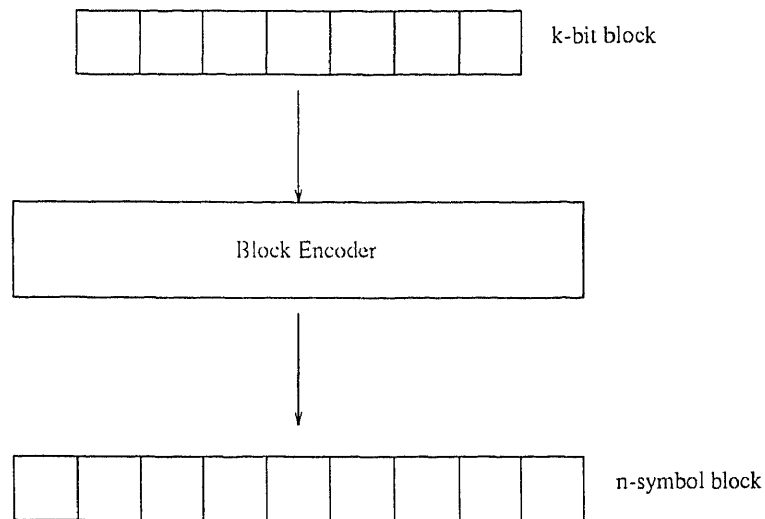


Figure 2.9 The fundamentals of block coding.

a vector of coded sequences, $C = \{C_0, C_1, C_2, \dots, C_m\}$. The mapping is carried out is one-to-one. This idea is shown in fig 2.9.

As opposed to block codes, which requires that the data bits are formatted into blocks, convolutional codes take a semi-infinite bit stream as their input and encode each bit on an individual basis. Redundancy can be introduced to the bit stream by means of a simple shift-register structure [17]. There are two fundamental parameters used to describe a convolutional code. The first is the code rate, R , defined as the number of bits entering the encoder, k , divided by the number of bits output by the encoder, n . Therefore, $R = k/n$. The second is the *constraint-length*, K of the code which is 1 plus the number of past inputs affecting current outputs. To illustrate the exact meaning of these parameters, we will consider the simple example of a rate-1/2 code as shown in fig 2.10. The shift register in this example can take on 4 states. So we can call this encoder a *4-state encoder*. We also show in fig 2.11 a more complicated encoder structure which generates a rate-1/3 code with a constraint length of 9. This encoder can also be called a 256-state encoder. This code has

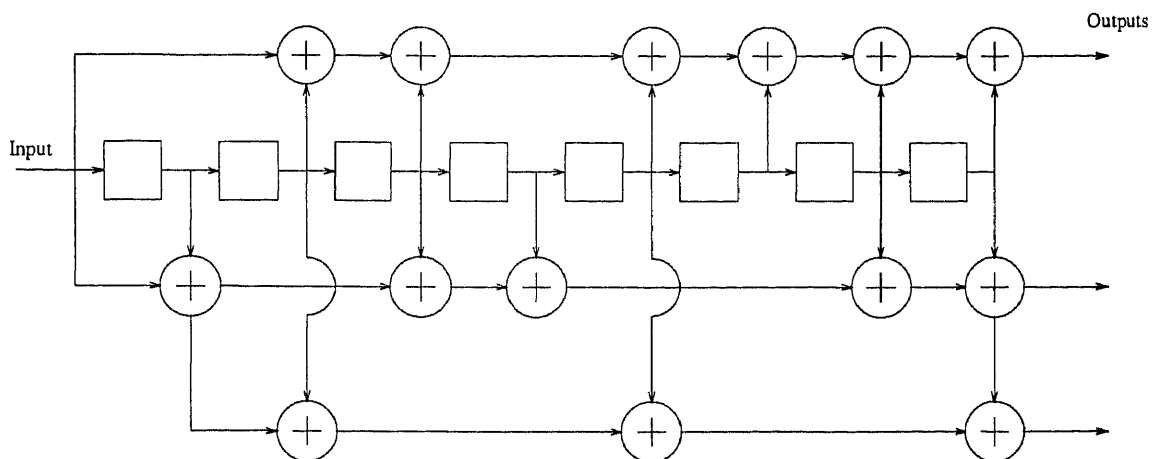


Figure 2.11 A 256-state convolutional encoder

the maximum number of guaranteed correctable errors per received codeword. It is written as

$$t = \left\lfloor \frac{d_{min} - 1}{2} \right\rfloor \quad (2.8)$$

where the notation $\lfloor x \rfloor$ stands for the “largest integer not to exceed x ” [14]. The parameter d_{min} is known as the *minimum distance* of the code.

A notion of minimum distance can be explained as in fig 2.12. In this example, we have two codewords, \mathbf{A} and \mathbf{B} , which have been shown on a number line calibrated in a distance metric called *Hamming distance*. A brief description of the Hamming distance is in order here. The Hamming distance between two codewords is simply the number of bit positions where they differ. For example, the Hamming distance between the codewords 000 and 011 is 2. The figure can be considered as a signal constellation, with every point between \mathbf{A} and \mathbf{B} representing an erroneous codeword. Assuming that \mathbf{A} was transmitted, the codeword received could be \mathbf{r}_1 , which means that 1 bit is in error. It may also be \mathbf{r}_2 , which means that 2 bits are in error (see fig 2.12). In both these cases, since the received codeword is closer (in terms of Hamming distance) to \mathbf{A} , the decoder will decide in favor of \mathbf{A} and thereby correct

the errors. However, if \mathbf{r}_3 is received when \mathbf{A} was transmitted, then the decoder will decide in favor of \mathbf{B} . This is an example of an *uncorrectable* error pattern. From this, we can see that this code has a minimum distance $d_{min} = 5$. From equation 2.8 (and our own observations based on the example we just considered), this code can correct all possible sequences of $t = 1$ errors and can even correct certain sequences of $t + 1 = 2$ errors [14].

At first look, it might look as though we can only obtain so much error correction from the code of the preceding example; however, a closer examination of the signal constellation reveals otherwise. It becomes apparent that the error correction capability of the code can be improved if we subdivided the distance between the successive codeword points (see the fig 2.13). In practice, this would correspond to the demodulator providing multi-level quantized outputs to the decoder for processing. In the fig 2.13, we show 3-bit quantization. The main idea here is to provide the decoder with more information for the decoding. Therefore, the distance metric that we are using here is the 3-bit quantized soft-decision metric. Obviously, the best distance metric would be the infinitely quantized soft-decision metric. However, this is difficult to implement in dedicated digital circuitry because the decoder would need to implement the soft decision metric

$$d = \sum_{k=1}^N (r_k - s_k)^2 \quad (2.9)$$

where r_k is the k-th component of the received code vector, s_k is the k-th component of the reference codeword that the received codeword is being compared to and N is the length of the code. This metric would need to implement N floating-point operations so it isn't used often. Usually, the metric implemented is usually the hard-decision metric (two-level quantization) or the soft-decision metric with 3-bit quantization.

The preceding discussion leads us to the most fundamental starting point in the study of decoding algorithms, that of *maximum-likelihood decoding*. This is

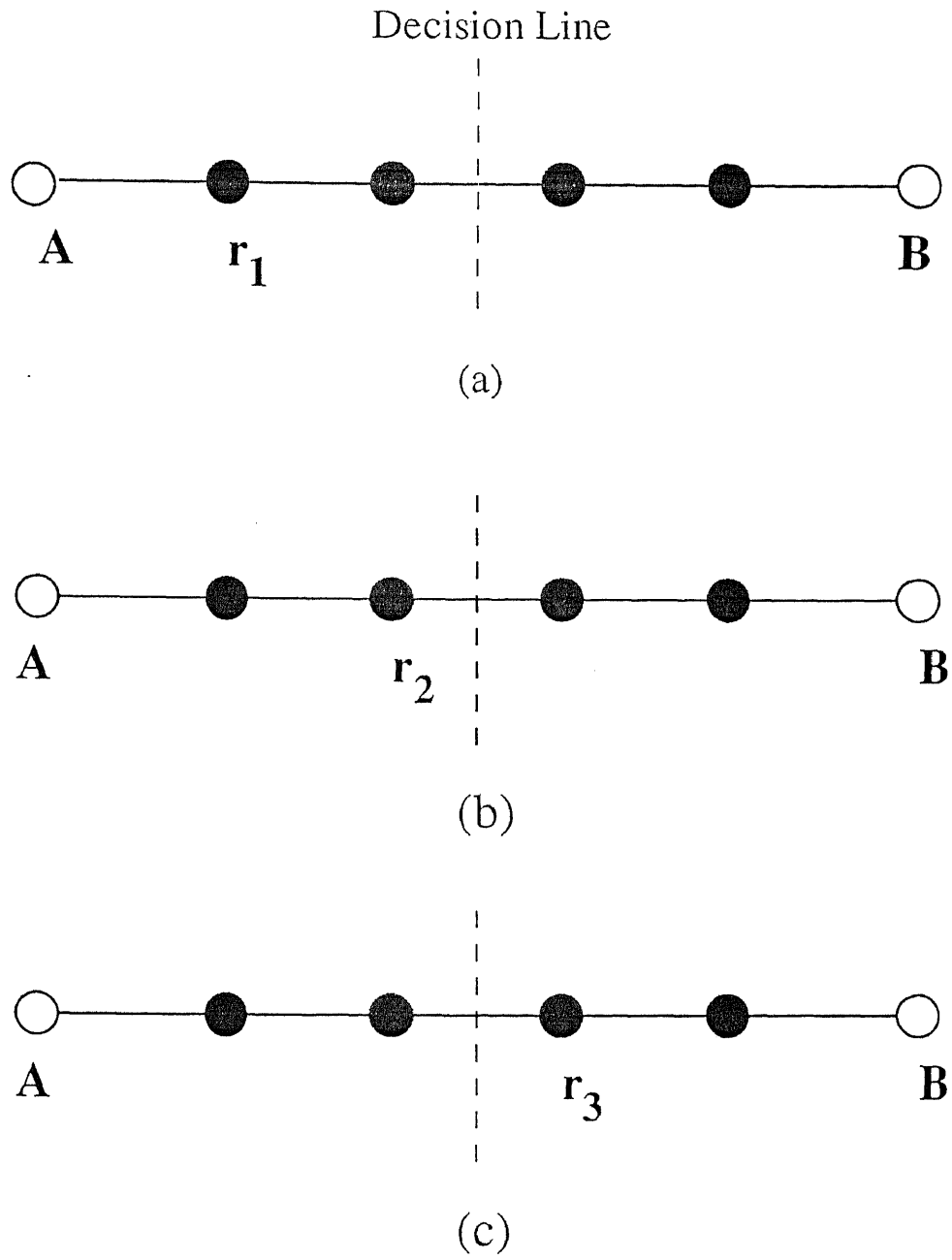


Figure 2.12 The concept of free distance

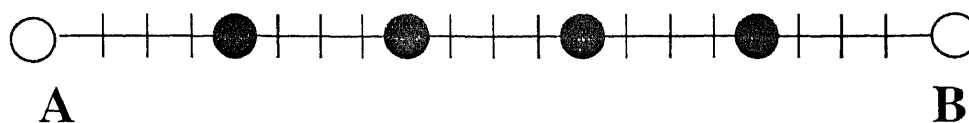


Figure 2.13 The concept of soft-decision decoding

an area that has been extensively treated by a number of authors [14], [3], [12], [17]. Therefore, we will only outline the fundamental ideas. A maximum-likelihood decoder simply tries to find a bit sequence, among all possible bit sequences, that most closely resembles the received sequence (in the context of minimizing the distance metric or maximizing the maximum-likelihood metric). At first look, it may appear as though this is not a viable approach and that a decoder that tries to predict the actual transmitted bits would be better. Even though it is possible to find decoding algorithms that use this latter approach, these have not resulted in decoder structures that can be implemented [3]. Therefore, maximum-likelihood decoding has become the prevalent starting-point for designing decoding algorithms, both for block codes and convolutional codes.

Before describing the Viterbi algorithm in detail, we must introduce the concept of a *code trellis*, which is an extremely convenient way of describing convolutional codes. Recall that convolutional encoders are based on a shift-register structure. This allows the encoder to be described, like any other sequential logic circuit, as a finite-state machine. The number of states is 2^{K-1} , where K is the constraint length. Whenever a new bit is input to the encoder, it causes a state transition. This is illustrated in fig 2.14. for the simple rate-1/2, $K = 3$ encoder illustrated in fig 2.10.

Although the state diagram is a perfectly acceptable way of describing the encoder, the same information can be conveyed in a better way by including the dimension of time. Another diagram, called the *trellis diagram* is used to do this.

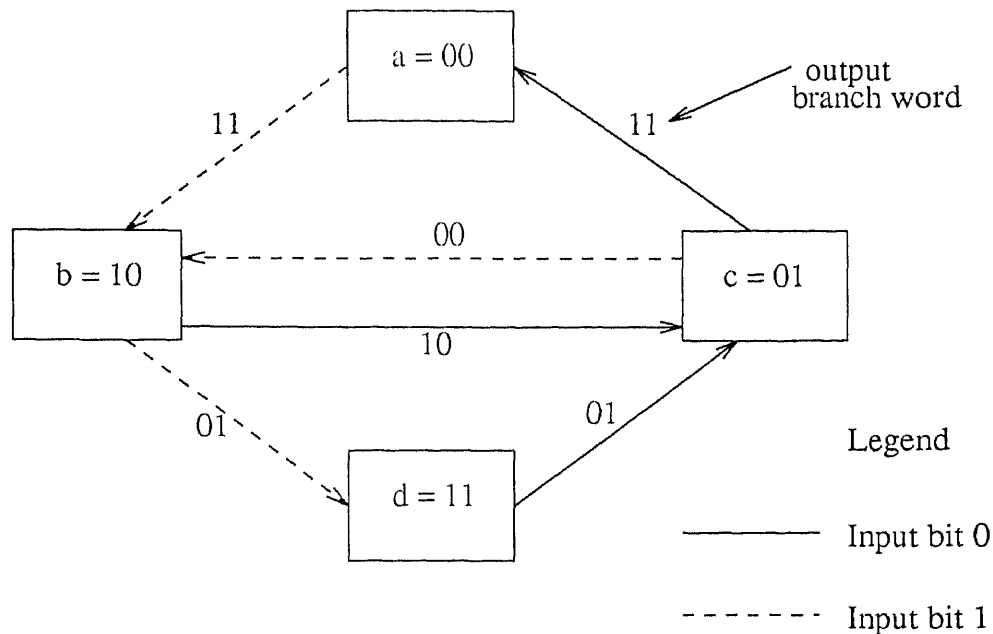
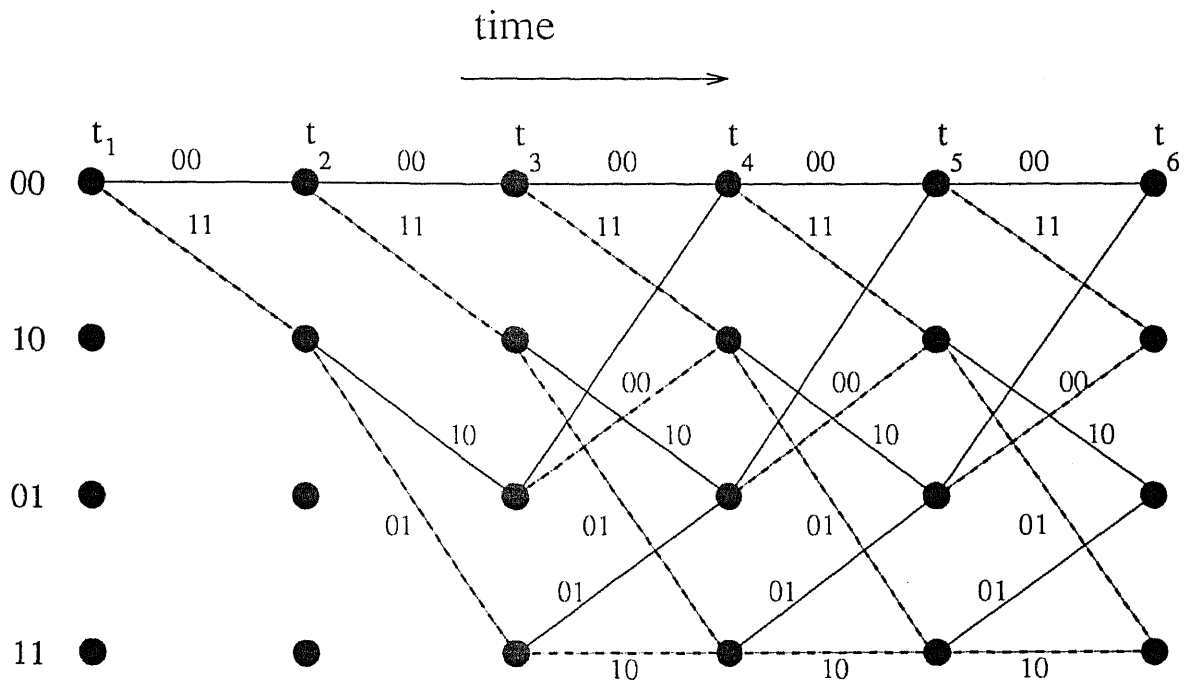


Figure 2.14 State diagram for a rate-1/2, $K = 3$ convolutional encoder

In fig 2.15 we show the trellis structure for the rate-1/2, $K = 3$ code (actually, the concept of a trellis is not unique to convolutional codes. Convolutional codes belong to a more general set of codes known as *trellis codes*, all of which can be described in terms of the same schematic structure).

Now we are ready to start our discussion of the Viterbi algorithm. As we have already mentioned, the algorithm is an example of maximum-likelihood decoding. Although first proposed by Viterbi in 1967, the technique itself was known in the field of operations research as an instance of *forward dynamic programming* [5]. Generally, the algorithm tries to find the optimal path through the trellis that maximizes the likelihood metric (or equivalently, minimizes the distance metric). As we have already discussed above, there are different distance metrics that can be used. The algorithm does not put any restrictions on the type of the metrics used. However, the performance of a Viterbi decoder improves with soft-decision metrics. The really attractive property of this algorithm is that the complexity of the decoder is not



Legend

----- Input bit 1

————— Input bit 0

Figure 2.15 Trellis diagram for the 4-state encoder

dependent on the number of symbols in the received codeword sequence. As we can see from the trellis diagram of fig 2.15, some of the paths in the trellis merge. The algorithm looks at all the paths and, at each time instant, discards the paths that cannot be part of the optimal path.

We now give a step-by-step definition of this algorithm. This definition was first given in [12]. Because of its brevity and clarity, we reproduce it here. In this description, N is the total number of information bits processed by the encoder and m is the number of zeros required to clear the encoder of all information bits ($K - 1$ zeros will be required).

step 1: *Begin at time instant $t = 1$. Compute the distance metric for the single path that enters each state. Store the paths and their cumulative path metrics for each state.*

step 2: *Increase t by 1. Compute the cumulative distance metric for all the paths entering the state by adding the branch metrics to the cumulative path metrics of the connecting survivor computed in the previous time instant. For each state, store the path with the minimum metric (the survivor) along with its metric, and eliminate all the other paths (as they cannot be part of the optimal path).*

step 3: *If $t < N + m$, repeat step 2. Otherwise, stop.*

There is one final aspect of error-control coding that is relevant to our discussion of CDMA systems. This is the subject of *interleaving*. To introduce the motivation for interleaving, we first note that all error-control coding algorithms are designed to detect and correct *random* errors introduced by the channel. However, in a mobile radio channel, sudden deep fades can cause errors to occur in bursts, rather than as isolated, random events. Interleaving is the re-arrangement of the data bits in time to break up the burst of errors so as to make them look like random errors. In this way, the errors can be corrected by the decoder.

1	7	13	19	25	31	37	43
2	8	14	20	26	32	38	44
3	9	15	21	27	33	39	45
4	10	16	22	28	34	40	46
5	11	17	23	29	35	41	47
6	12	18	24	30	36	42	48

Output symbols : 1,7,13,19,25,31,37,43.....

Figure 2.16 The block interleaver

There are two types of interleaving: *block interleaving* and *convolutional interleaving*. Neither has any significant advantages over the other. Nevertheless, block interleaving seems to be preferred for virtually all wireless cellular systems, including CDMA. Therefore, we shall neglect convolutional interleaving and talk about block interleaving instead.

In a block interleaver, there is a memory array which has M rows by N columns. The symbols are written to the memory arrays by columns and read out by rows as shown in fig 2.16. In the deinterleaver (see fig 2.16), the reverse operation will be performed, that is, the symbols are written to the array by rows and read out in columns. To see the functionality of this technique, assume that the channel has introduced a burst of errors on the symbols 7, 13, 19 and 25 (see fig 2.16). As we can see from fig 2.17, at the output of the deinterleaver, the burst of errors will appear to the decoder as they were random errors.

1	7	13	19	25	31	37	43
2	8	14	20	26	32	38	44
3	9	15	21	27	33	39	45
4	10	16	22	28	34	40	46
5	11	17	23	29	35	41	47
6	12	18	24	30	36	42	48

Output symbols: 1,2,3,4,5,6,7,8,9,10,11,12,13,14,15,16,17,19,20,21,22,23,24,25,.....

Figure 2.17 The block deinterleaver

To conclude our discussion, we briefly examine some important characteristics of block interleaving. First, we note that any burst of N erroneous symbols will appear at the deinterleaver output as separated from each other by at least M symbols [14]. Secondly, the minimum delay produced by the interleaver-deinterleaver combination is $(2MN - 2M + 2)$ symbol times, not including any other extra delays produced by the channel. Thirdly, for practical purposes, we note the memory requirements. Generally, we would need to use $2M \times N$ memory arrays to implement both the interleaver and the deinterleaver so that one $M \times N$ array can be read while other is being written to and vice versa.

CHAPTER 3

SIMULATION RESULTS

3.1 Chapter Overview

In this chapter, the simulator developed will be used to simulate some familiar system scenarios. We shall examine the results in detail and comment on them briefly.

3.2 Simulation Results

For the first simulation, we consider the overall effects of coding on a multiuser system. Here we simulate a two-user system, with each user employing DS/BPSK modulation, with and without error-correction coding. The code used is a 4-state, rate-1/2 convolutional code whose structure was already presented in the previous chapter. This same code is used throughout the other simulations. A Viterbi decoder with hard-decision inputs is used at the receiver for the decoding.

For the second simulation, we simulate the effects of varying the correlation coefficient (and hence the multiple-access interference) on a two-user DS/CDMA uplink. We observe and plot the error performance of the desired user (arbitrarily taken as user 1). The results are shown in fig 3.2.

The third simulation is the same as the previous one. However, in this case a Viterbi decoder with infinitely-quantized soft-decision inputs is used for the decoding. We once again present the error performance of the desired user as in fig 3.3.

The next two simulations involve the effects of path-loss on the error performance of the desired user. The simulation is performed by scaling the power of the desired user (user 1 in this case) by a path-loss parameter α defined by:

$$\alpha = \left(\frac{d_1}{d_2} \right)^n \tag{3.1}$$

where d_1 and d_2 represent the distances (normalized with respect to the radius of the cell) of the first user and the second user respectively. n is a factor which

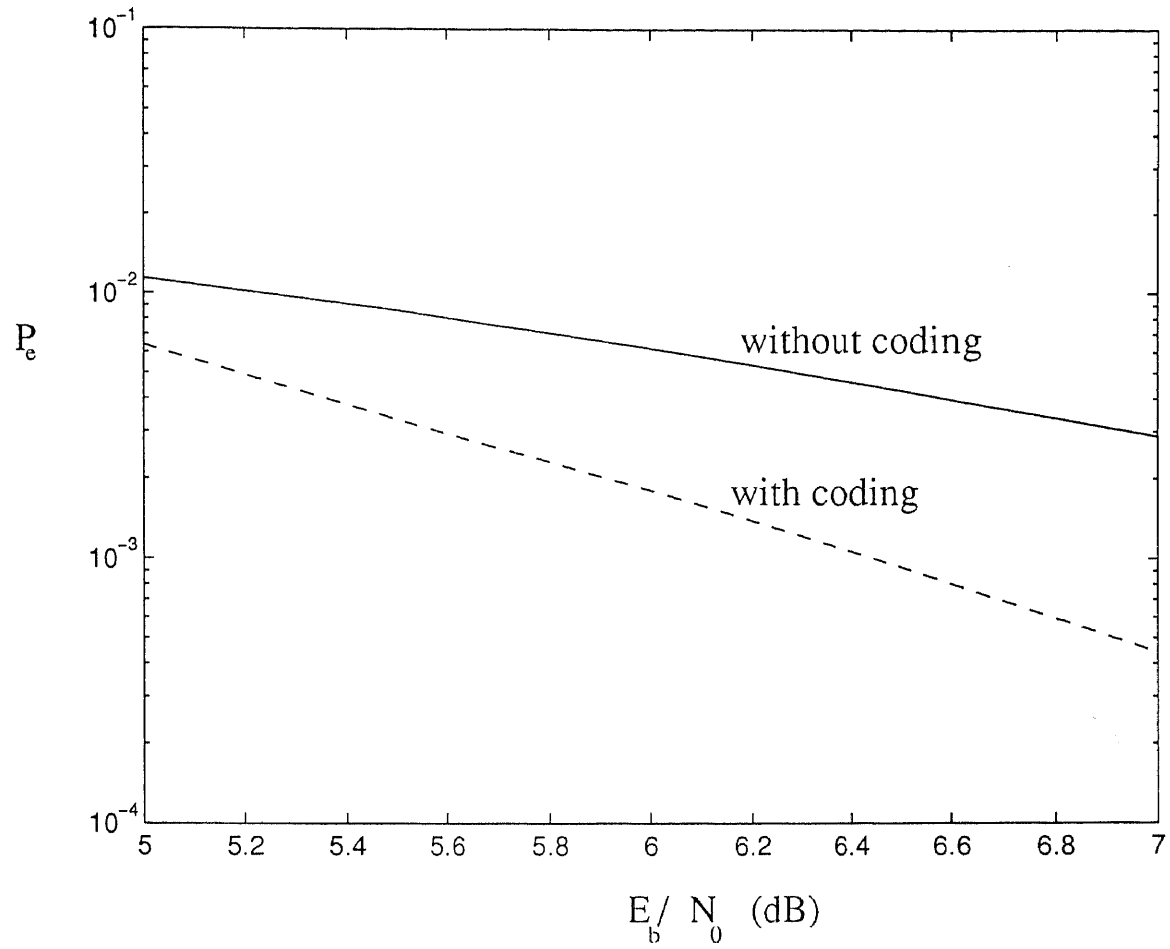


Figure 3.1 A two-user simulation with and without error-control coding

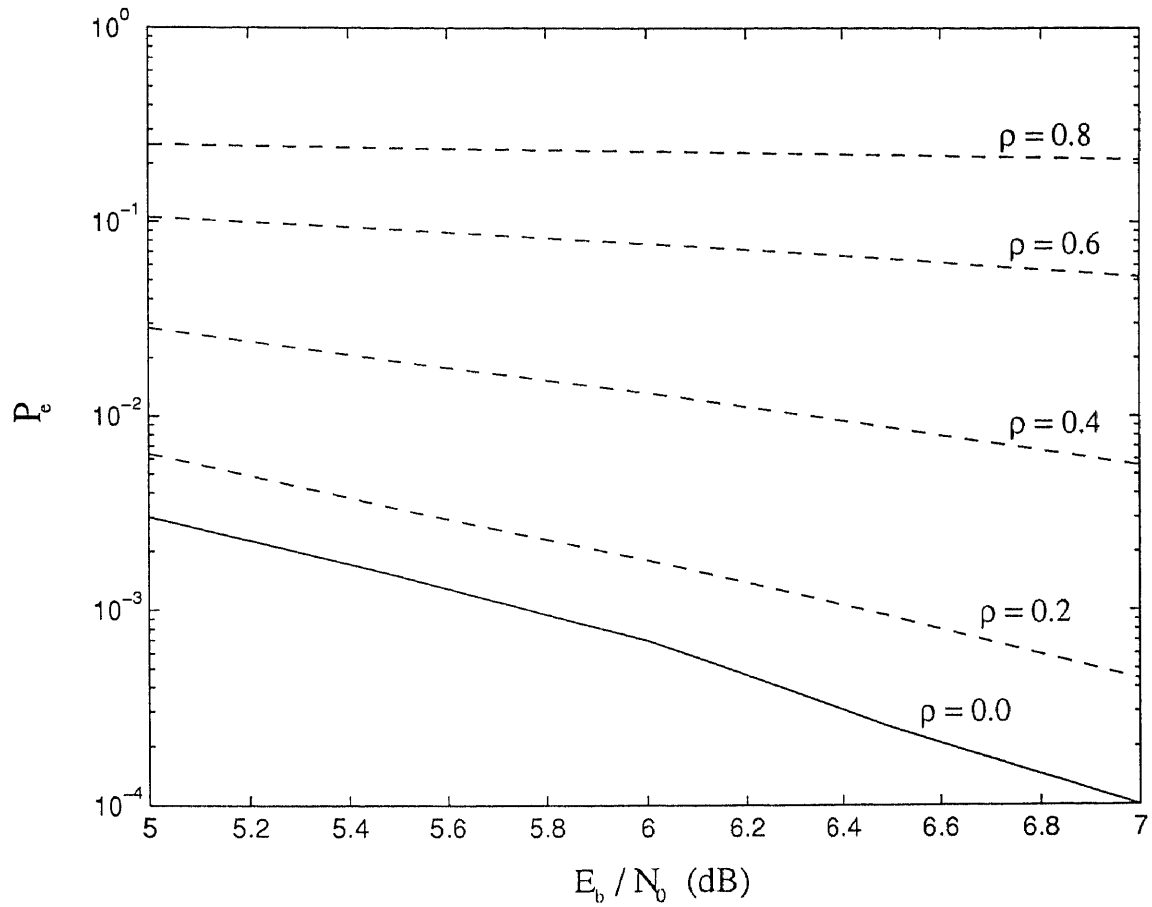


Figure 3.2 Error performance of the desired user with differing levels of multiple-access interference (hard-decision decoding)

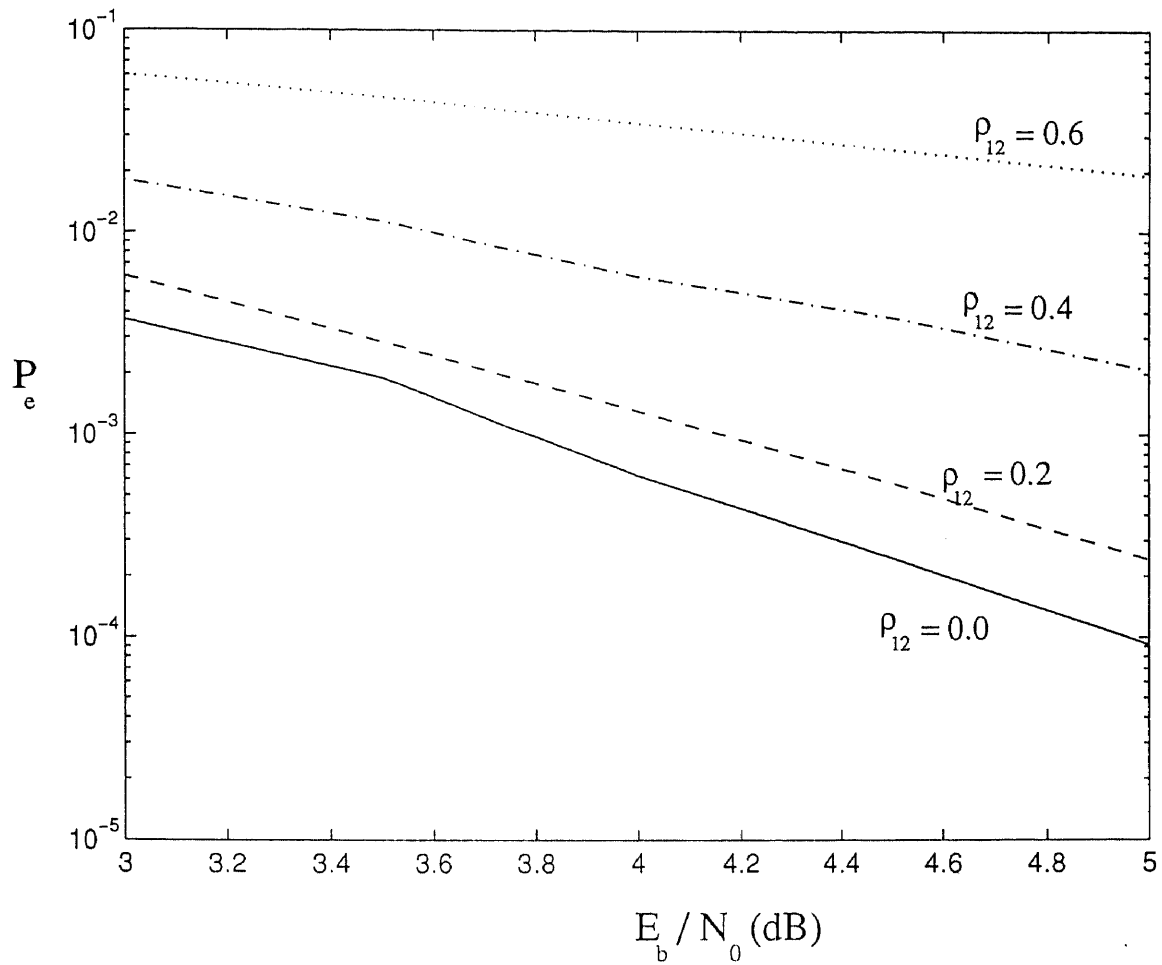


Figure 3.3 Error performance of the desired user with differing levels of multiple-access interference (soft-decision decoding)

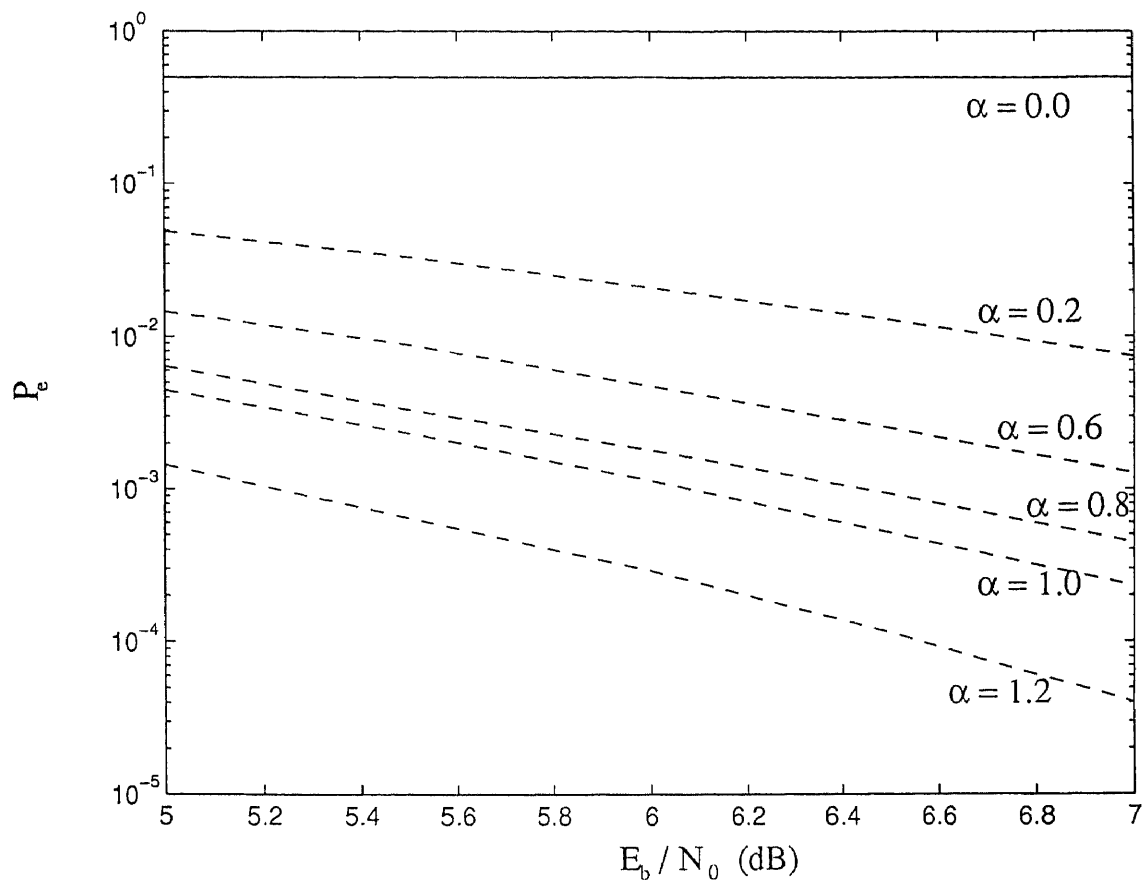


Figure 3.4 Error performance of the desired user with differing levels of path-loss (hard-decision decoding)

represents the propagation characteristics of the channel, which can be between 2 and 4 for most practical cases. We have taken $n = 2$ for our simulations. The results are presented for both hard-decision and soft-decision decoding. The results are presented in figs 3.4 and 3.5.

We finally present the results of a multiple-user simulation. In this simulation, we investigate the effects of multiple-access interference in a multiple-access environment with more than two users. Each user is assigned a different cross-correlation coefficient. The coefficients are taken from the elements of the cross-correlation matrix of a length-seven Gold code. The results are shown in fig 3.6.

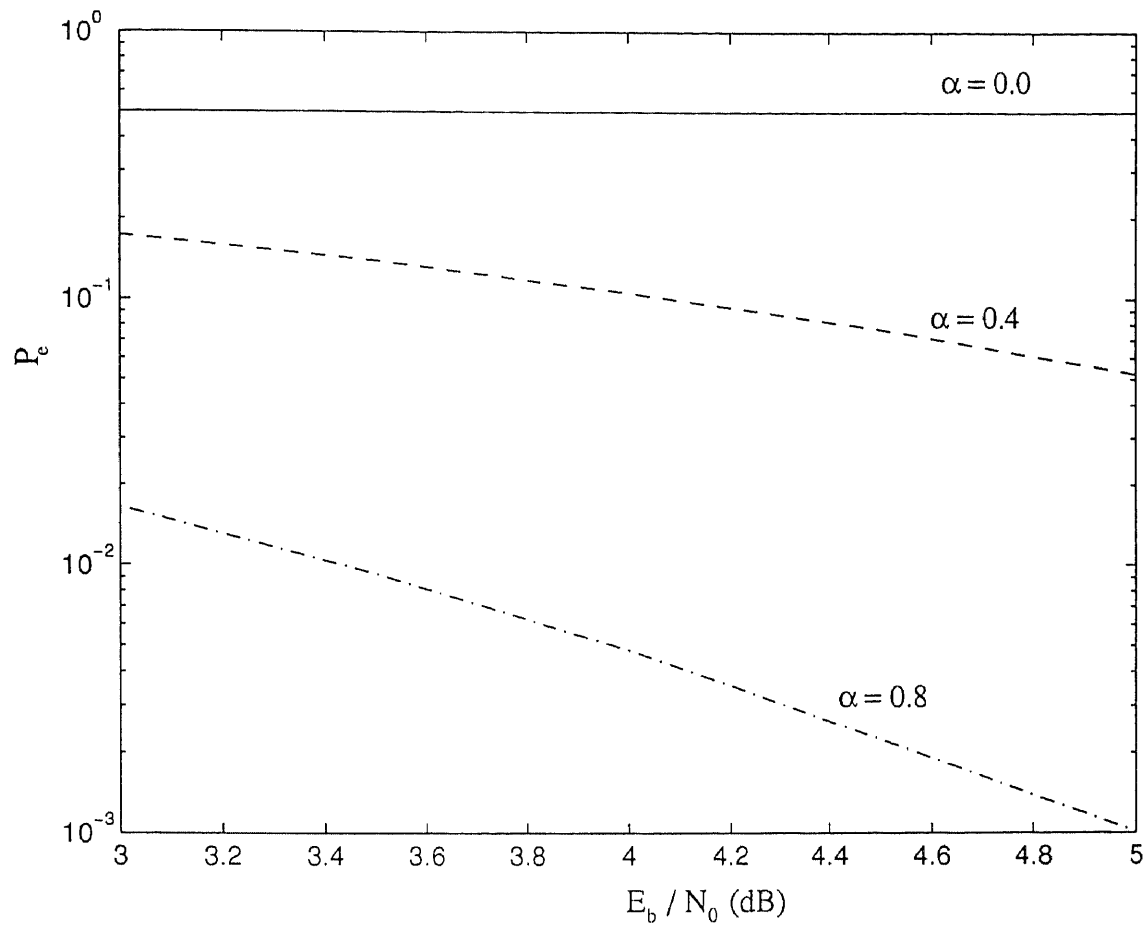


Figure 3.5 Error performance of the desired user with differing levels of path-loss (soft-decision decoding)

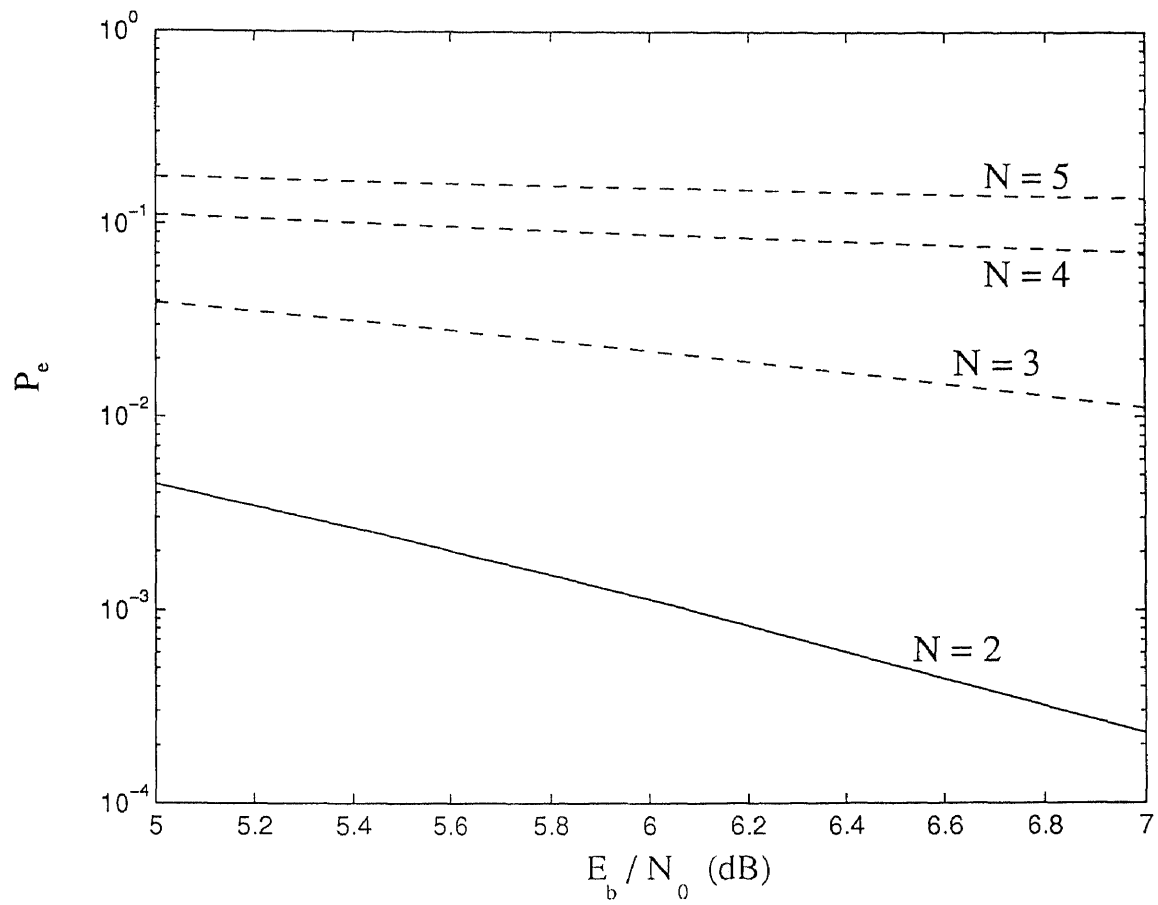


Figure 3.6 Error performance of the desired user in a multiuser environment

In the next chapter, we will briefly comment on these results and their significance as far as the functionality of the simulator is concerned. We shall also make some suggestions as to how the work may be extended.

CHAPTER 4

CONCLUSIONS & SUGGESTIONS FOR FURTHER WORK

4.1 Chapter Overview

In this chapter, we shall briefly comment on the simulation results and their significance. We shall also put forward a few suggestions as to how this work may be extended.

4.2 Conclusions on Results

As already mentioned in the previous chapter, the simulations in the previous chapter were carried out with the sole aim of testing the functionality of the simulator and seeing whether it produces the results that are expected. The results clearly suggest that the simulator is fully functional and does produce correct results. Furthermore, the general trend displayed by the results also supports our intuitive opinions regarding them. For instance, in the simulations of multiple-access interference effects with two users, it is obvious that as the correlation coefficient ρ_{12} between the user signature sequences is increased, the error performance of the desired user (arbitrarily assumed as user 1) will worsen. Similarly, in the simulations of path-loss effects, it is apparent that as the desired user gets closer to the base station, its signal will be received at a higher level compared to the interfering user and this will affect the error performance of the desired user favorably. For a two-user case, it is also apparent that coded modulation is more effective than uncoded modulation for the purpose of combating (although to a limited extent) multiple-access interference. Lastly, for the multiple-user simulation, it is obvious that the error performance of the desired user will degrade as the number of users are increased because this will increase the multiple-access interference experienced by the desired user. Because of these results, our overall conclusion is that this simulator is fully functional and is capable of handling simulations of more advanced system scenarios.

4.3 Suggestions for Further Work

As we already mentioned in chapter 1, the main aim was to develop a flexible simulator capable of handling different simulation scenarios. While the simulator in its present state does not have many advanced features, its modular design allows plenty of room for further development. We believe that a few of the areas where the simulator can be extended are the following:

- Implementation of realistic fading channel models and their effects on performance.
- Implementation of models for shadowing phenomena (such as log-normal shadowing) and their effects on performance.
- Implementation of various power control algorithms.
- Extension of the simulator to the multiple-cell case with some emphasis on network-level protocols.

REFERENCES

1. A. J. Viterbi, A. M. Viterbi, and E. Zehavi, "Performance of Power-Controlled Wideband Terrestrial Digital Communication," *IEEE Transactions in Vehicular Technology*, vol. 41, no. 4, pp. 558-569, April 1993.
2. P. T. Brady, "A statistical analysis of on-off patterns in 16 conversations," *Bell System Technical Journal*, vol. 47, pp. 73-91, January 1968.
3. G. C. Clark and J. B. Cain, *Error-Correction Coding for Digital Communications*, Plenum, New York, 1981.
4. H. Taub and D. L. Schilling, *Principles Of Communication Systems*, McGraw-Hill, New York, NY, 1986.
5. J. D. Gibson, *Principles of Digital and Analog Communications*, Macmillan, New York, 2nd ed., 1993.
6. K. S. Gilhousen, I. M. Jacobs, R. Padovani, A. J. Viterbi, L. A. Weaver Jr. and C. E. Wheatley III, "On the Capacity of a Cellular CDMA System," *IEEE Transactions on Vehicular Technology*, vol. 40, no. 2, pp. 303-312, May 1991.
7. W. C. Y. Lee, "Overview of Cellular CDMA," *IEEE Transactions on Vehicular Technology*, vol. 40, no. 2, pp. 291-302, May 1991.
8. J. G. Proakis, *Digital Communications*, McGraw-Hill, New York, 3rd ed., 1995.
9. R. L. Peterson, R. E. Ziemer and D. E. Borth, *Introduction to Spread Spectrum Communications*, Prentice-Hall, Englewood Cliffs, NJ, 1995.
10. R. L. Pickholtz, L. B. Milstein, and D. L. Schilling, "Spread Spectrum for Mobile Communications," *IEEE Transactions on Vehicular Technology*, vol. 40, no. 2, pp. 313-321, May 1991.
11. S. Haykin, *Communication Systems*, John Wiley and Sons, Inc., New York, NY, 3rd ed., 1994.
12. S. Lin and D. J. Costello, Jr., *Error Control Coding: Fundamentals and Applications*, Prentice-Hall, Englewood Cliffs, New Jersey, 1983.
13. A. Salmasi, "Cellular and Personal Communications Networks Based on the Application of Code Division Multiple Access (CDMA)," *Proceedings of the Virginia Tech Symposium on Personal and Mobile Communications*, 1990.
14. B. Sklar, *Digital Communications Fundamentals and Applications*, Prentice-Hall, Englewood Cliffs, New Jersey, 1988.

15. A. J. Viterbi, "Spread-spectrum communications: Myths and realities," *IEEE Communications Magazine*, vol. 12, pp. 11–18, May 1979.
16. D. P. Whipple, "The CDMA Standard," *Applied Microwave & Wireless*, pp. 24–39, Winter 1994.
17. S. B. Wicker, *Error Control Systems for Digital Communication Systems and Storage*, Prentice-Hall, Englewood Cliffs, New Jersey, 1995.